Iranian Journal of Pharmaceutical Sciences
2026: 22 (1): 180-191
https://journals.sbmu.ac.ir/IJPS

Research Article

OPEN ACCESS

Design of Experiment-Based Optimization in Formulation of Atorvastatin Solid Dispersion using *Linum usitatissimum* Seed Gum

Ramarao Bora[a], Satyalakshmi Siragam*[b]

[a] *Department of Pharmaceutical Sciences, School of Biotechnology and Pharmaceutical Sciences, Vignan's Foundation for Science, Technology and Research, Vadlamudi, Guntur-522213, Andhra Pradesh, India.*
[b] *Department of Pharmaceutics, Vignan Institute of Pharmaceutical Technology, Duvvada, Beside VSEZ, Visakhapatnam, Andhra Pradesh-530049, India.*

Received: July 22, 2025 **Last Revision:** October 18, 2025 **Accepted:** January 26, 2026 **Available online:** June 15, 2016.

Abstract

Solid dispersion (SD) is the most promising approach for enriching the drug release of poorly soluble drugs. Atorvastatin (ATR) is a lipid-lowering drug, but its low water solubility hinders its dissolution and effective treatment. In this study, flaxseed gum (FSG) derived from *Linum usitatissimum* has been investigated as a potential carrier for SD formulations to overcome solubility limitations. A modified hot extraction procedure was employed to isolate FSG, which was subsequently characterised for its physical properties. Design of experiments was conducted using Response Surface Methodology (RSM), with FSG concentration, solvent volume, and temperature as independent variables to optimize the SD formulation via the solvent evaporation technique (SEV).

In contrast, the percentage of drug release in 30 minutes serves as the response variable. The formulations were assessed for product quality parameters, and the optimized SD formulation was characterized physicochemically. 33.8 mg of FSG, 8 mL of solvent (ethanol), and 42.5°C were identified as critical quality attributes through RSM. The optimized ATR-SDs formulation exhibited 92% drug release in 30 minutes, 98% drug content, and 1.53-fold improved solubility than pure ATS. Differential scanning calorimetry and x-ray diffraction analysis showed that the drug crystalline form transformed to an amorphous state, while scanning electron microscopy images revealed increased porosity in SD. The current research has demonstrated that the SD of ATR employing a natural carrier could be a promising formulation for enhancing solubility and dissolution.

Keywords: Atorvastatin; Solid dispersion; Design of experiments; *Linum usitatissimum*; Solubility enhancement; Solvent evaporation.

1. Introduction

About 40% of approved drugs and nearly 90% of drug candidates are poorly water-soluble [1]. The drug's low solubility impairs its dissolution, resulting in inadequate blood concentrations. Typically, this issue is addressed by increasing the dosage, however, this approach is associated with few limitations such as adverse reactions, high treatment expenses, and patient non-

*** Corresponding Author**:
S Satyalakshmi, Department of Pharmaceutics, Vignan Institute of Pharmaceutical Technology, Visakhapatnam-530049, Andhra Pradesh, India.. E-mail: satyalaxmi148@gmail.com; lakshmisiragam48@gmail.com.

Cite this article as: Rama Rao B., Satyalakshmi S. Design of Experiment-Based Optimization in Formulation of Atorvastatin Solid Dispersion using *Linum usitatissimum* Seed Gum. Iran. J. Pharm. Sci., 2026, 22 (1): 180- 191.

DOI: https://doi.org/10.22037/ijps.v22i1.49175

This open-access article is distributed under the terms of the Creative Commons Attribution Non Commercial 4.0 License (CC BY-NC 4.0).

compliance [2]. Methods that conventionally employed to address the limitations of poorly water-soluble drugs typically involve micronization, salt formation, the use of surfactants, nanocarriers, and prodrugs [3-8]. Despite their utility, these methods have inherent limitations. SDs are the most effective in enhancement of solubility by reducing particle size, expanding surface area, improving wettability, and increasing the amorphous state of the water-insoluble compound. Malkawi *et al*. listed various marketed solid dispersion formulations used for the treatment of conditions such as cancer, immune-related disorders, and viral and fungal infections [9]. Natural polymers are more attractive carriers for solid dispersions because they are biodegradable, break down into harmless substances, allow controlled release of the drug, and exhibit minimal side effects [10].

Numerous plant-derived pharmaceutical excipients are widely used in the pharmaceutical industry [11]. Given that vegetable sources are sustainable and can be cultivated and harvested in an environmentally friendly manner, a reliable and ongoing supply of raw materials is ensured. Substances derived from plants can pose some challenges, including limited biosynthesis in small quantities and complex structures that vary depending on factors such as the plant's location and seasonal fluctuations. Challenges include slow and expensive isolation and cleaning process [12].

Natural gums comprise polysaccharides with a significant number of sugar units, which are linked together to create large molecules. Polysaccharides exhibit hydrophilic properties, demonstrate robust stability after absorption, and are enzymatically degradable, characteristics that distinguish them from synthetic polymers. Natural polysaccharides are suitable for a range of biomedical applications due to their biocompatibility, non-toxicity, low allergenicity, biodegradability, and chemical flexibility [13, 14]. Consequently, Naturapolyceutics, a new concept, enables the creation of a technology platform that combines natural polymers and pharmaceuticals to design and develop drug delivery systems [15].

FSG is extracted from linseed hulls by soaking the seeds in distilled water. FSG is a complex polysaccharide primarily composed of neutral and acidic fractions [16], which play a crucial role in enhancing the solubility of poorly soluble drugs in SD. The key chemical components responsible for this enhancement are: arabinoxylans branched polysaccharides containing arabinose and xylose units, which improve water absorption and wettability [17]. Rhamnogalacturonans-pectic polysaccharides contain rhamnose, galactose, and uronic acids, which promote water retention and create a hydrophilic environment. Mucilage & Galactomannans-high molecular weight polymers form hydrated gels, facilitating drug dispersion and preventing crystallization [18, 19]. FSG has been used in previous studies as a thickening agent, in the formulation of bio-composite hydrogel films, and in floating drug delivery systems [20-22]. HMG-CoA reductase, a crucial enzyme in cholesterol biosynthesis, is effectively inhibited by ATS. ATS has a very low solubility in simulated gastric medium, at less than 0.1 mg/mL, and its solubility is extremely low in both distilled water (ranging from 0.11 to 0.2 mg/mL) and phosphate buffer pH 6.8 (with a solubility range of 0.29-0.32 mg/mL) [23, 24]. ATS has a low oral bioavailability of 12%, primarily due to its low water solubility, crystalline structure, and hydrophobic properties, as well as rapid removal of the drug from the bloodstream during its initial passage through the gut wall and the liver before it reaches systemic circulation. The development of SDs enhances the solubility and dissolution rate of solids and has been shown to increase their bioavailability. ATS, when formulated in supersaturated solutions, exhibits a strong tendency for particles to stick together, impairing its wettability and accelerating recrystallization during dissolution studies. Currently, hydrophilic polymers are used as carriers in solid dispersions due to their high hydrophilicity, water-absorption capacity, and plasticizing effect [25].

The current study reports the optimization of formulation parameters for the preparation of ATR-SDs using a design of experiments (DoE). A central composite design was used, with formulation factors as independent variables and the critical quality attributes (CQAs) of ATR-SDs as response variables. The developed SD formulation was characterized for various physicochemical properties and evaluated for in *vitro* drug release.

2. Materials and methods

ATS was a gift from Hetero Drugs Pvt. Ltd., Ethanol (Analytical grade), and other materials used in the formulations were purchased from Merck Ltd., Mumbai.

This open-access article is distributed under the terms of the Creative Commons Attribution Non Commercial 4.0 License (CC BY-NC 4.0).

2.1. Extraction and characterization of FSG

First, the flax seeds are mixed with water at a 1:20 (w/v) ratio. The mixture is then stirred for 0.5 to 8 hours at a controlled temperature not exceeding 50°C. Following stirring, the mucilage extract is separated from the solid residue using filtration by a clean cloth or strainer. To precipitate the mucilage from the concentrated solution, it is treated with a mixture of 80% ethanol and water (1:4 v/v). After allowing the precipitate to stand for 1 hour at a low temperature, and then collected by centrifugation at 6000 rpm for 30 minutes. The collected precipitate is dried and characterized [26].

2.2. Characterization of FSG [21, 25]

2.2.1. Percentage yield of FSG

The FSG yield was determined using Equation 1, and the associated mean error was calculated for this process.

$$\%\ \text{of yield} = \frac{\text{Weight of mucilage in g}}{\text{Weight of seeds in g}} \times 100 \qquad (1)$$

2.2.2. Swelling index

One gram of FSG powder was precisely measured and placed into a 100 mL stoppered measuring cylinder. The initial volume of the powder in the measuring cylinder was recorded. The volume was brought up to 100 mL using distilled water. The gum sediment was then gently agitated and placed in a sealed container for 24 hours at a temperature consistent with room temperature and a relative humidity typical of the ambient environment. The volume of the gum sediment was recorded after 24 hours. The swelling ability of FSG was quantified using the swelling index. The swelling index was represented as a percentage and computed using the following formula.

$$\text{SI} = \frac{\text{Ht} - \text{Ho}}{\text{Ho}} \times 100 \qquad (2)$$

The initial height of the powder in the graduated cylinder is denoted as Ho, while Ht represents the height taken up by the swollen gum after 24 hours.

2.2.3. Viscosity measurement

The viscosity of a 1 % (w/v) FSG solution was measured using a Brookfield LVDV+PRO viscometer in accordance with USP guidelines.

2.2.4. Angle of repose

The angle of repose was determined using the funnel method. The powder was funnelled after it had been accurately weighed. The funnel's height was adjusted so that its tip contacted the summit of the powder pile. The powder was permitted to flow freely through the funnel onto the surface [27]. The diameter of the powder heap was determined, and the angle of repose was calculated using the following equation:

$$\tan(\theta) = \frac{\text{H}}{\text{R}} \qquad (3)$$

H-Height of powder heap; R-Radius of powder heap.

2.2.5. Moisture sorption capacity

An experiment to investigate moisture sorption was conducted in an incubator setting. A uniform layer of powdered FSG was spread across a 9 cm-diameter petri dish, with a total of 1 gram of the substance. The sample was then maintained in an incubator at a 37±1°C for the duration of 2 days. The sample's weight was monitored before and after exposure to incubator temperature to determine moisture sorption.

2.2.6. Hydration capacity

The hydration capacity was determined as follows. A quantity of gum powder was measured and placed in a 15 mL centrifuge tube. Next, 10 mL of distilled water was added, and the mixture was centrifuged for 10 minutes at 1,000 revolutions per minute. After centrifugation, the blank centrifuge tube was removed and inverted to discard the remaining liquid. The tube that had been decanted was then weighed, and the hydration capacity was determined using the equation listed below.

$$HC = \frac{\text{Weight of the hydrated sample}}{\text{Weight of dry sample}} \qquad (4)$$

2.2.7. Density

The loose and tapped bulk densities of FSG were measured. A calibrated measuring cylinder (10 mL capacity) was filled with 2 gm of powdered gum, and the initial volume was recorded. The cylinder was then permitted to drop from a height of 2.5 cm onto a hard surface at a 2-second interval. The tapping was continued until no further change in volume was observed. The LBD and TBD were calculated using the equation:

$$LBD = \frac{\text{Weight of the powder}}{\text{Volume of the packing}} \qquad (5)$$

$$\text{TBD} = \frac{\text{Weight of the powder}}{\text{Tapped volume of the packing}} \qquad (6)$$

This open-access article is distributed under the terms of the Creative Commons Attribution Non Commercial 4.0 License (CC BY-NC 4.0).

2.2.8. Compressibility

Compressibility index (Carr's index) was determined by using the following equation:

$$\text{Carr's index } (\%) = \frac{(\text{TBD}-\text{LBD})}{\text{TBD}} \text{X}100 \quad (7)$$

2.2.9. Basic physicochemical composition of FSG

Aqueous extract was prepared by suspending FSG powder in distilled water. Crude protein, crude fat, total carbohydrate, moisture, and ash contents of the isolated gum were determined [12, 17, 28].

2.3. DoE optimization of preparation parameters for ATR-SDs

2.3.1. Experimental design

Design Expert 12 (Stat-Ease Inc., Minneapolis) was used to formulate ATR-SDs, selecting a three-factor, three-level central composite design (CCD). The amount of FSG (F1), solvent (ethanol) (F2), and temperature (F3) were selected as three factors. % of drug release at 30 minutes was taken as the response variable and shown in **Table 1** [29]. A trail of 20 experiments was constructed. The results were analyzed using multiple regression.

Table 1. Variables selected for the three-level factorial design

Factors	Units	Coded values	
		+1	-1
A: FSG	Mg	10	50
B: Ethanol	mL	1	15
C: Temperature	^{o}C	35	50

2.4. Preparation of SD using purified FSG as a carrier

SDs by SEV were made as per the experimental runs developed by DoE shown in **Table 2**. A fixed amount of ATR (10 mg) and varying amounts of carrier, as per the design, were dissolved in the smallest possible volume of methanol, then the solution was evaporated below 50°C to obtain a dry powder. Finally stored in a dessicator.

Table 2. CCD with 20 experimental runs

Run	Factor A: FSG (mg)	Factor B: Solvent (mL)	Factor C: Temperature (^{o}C)	Y_2: % Release at 30minutes
1	30	8	42.5	89
2	50	15	35	78
3	50	1	50	75
4	10	1	50	70
5	30	8	42.5	88
6	30	8	35	83
7	50	1	35	72
8	**33.8**	**8**	**42.5**	**92**
9	30	8	42.5	88
10	30	8	42.5	89
11	30	15	42.5	85
12	10	8	42.5	79
13	10	15	50	73
14	50	15	50	74
15	10	1	35	71
16	10	15	35	75
17	30	8	42.5	89
18	30	8	50	82
19	30	1	42.5	80
20	50	8	42.5	78

This open-access article is distributed under the terms of the Creative Commons Attribution Non Commercial 4.0 License (CC BY-NC 4.0).

2.4.1. Characterization of SD

The flow behaviour of the prepared SD was evaluated. Entrapment efficiency (%), the practical yield of formulated SD, was determined [30].

2.4.1.1. Saturated solubility studies for SDs

Saturated solubility analysis of all the prepared SDs was performed by adding 10 mL of water to an excess amount of each SD. The prepared solution was placed in a shaker for 48 hours at room temperature, and then the samples were filtered using a 0.4 µm Whatman filter paper. The dissolved drug concentration was measured by UV spectrophotometry, and solubility was measured in triplicate. Based on solubility, the solid dispersion ratio of the drug with the polymer was selected for the formulation of immediate-release tablet dosage forms.

2.4.1.2. Drug content

The resulting SDs were weighed (SDs equivalent to 100 mg of drug) and dissolved in 100 mL of distilled water containing 1.5% tween 20. After the samples were filtered, the amount of drug was measured at 241 nm using spectrophotometry.

2.4.1.3. Dissolution studies

Using 0.1 M HCl (pH -1.2) as dissolution medium with 0.5% SLS (w/v) at 37 ± 0.5 °C and a type II USP dissolution test apparatus (Lab India, model- DS 8000) run at 100 rpm, the dissolution rates of the SDs equivalent to 100 mg of drug were determined. The dissolving medium was removed in 5 mL aliquots at different time intervals. The samples were analyzed spectrophotometrically at 241 nm after appropriate dilution. Surface morphology, drug carrier compatibility studies, and DSC and XRD were determined for the SDs showing high drug release.

2.4.1.4. Scanning electron microscopy (SEM)

All samples were taken with a scanning electron microscope (SEM-Model: JOEL- JSM 5600). Samples were placed over the stubs with double-sided carbon-conductivity tape, and a thin layer of gold was coated over the mounted samples using an automated sputter coater. The treated SD sample was scanned according to standard procedures at RUKSA Lab's College of Veterinary Science, SVVU, Rajendranagar, Hyderabad, India.

2.4.1.5. Differential scanning calorimetry (DSC)

The degree of change in the physical characteristics of SDs was assessed using a DSC (Q100 TA Instrument, Germany). Melting-point calculations were automatically performed for the pure drug and for the drug incorporated into the SD formulation.

2.4.1.6. Powder X-ray diffraction

The powder X-ray diffraction patterns of the samples were collected with a Rigaku Miniflex diffractometer (Rigaku Corporation, Tokyo, Japan) at 40 kV and 30 mA. The samples were analyzed over a 2θ range of 5-45° at a scanning rate of 2°/minutes using a CuKα radiation source.

2.4.1.7. Compatibility studies of drug excipients using Fourier transform infrared spectroscopy (FTIR)

The FTIR spectra of ATS and flaxseed gum used to prepare SD were obtained. The FTIR spectra were recorded by the KBr pellet method using the BRUKER FTIR INVIVO spectrometer from Japan. The infrared (IR) spectrum was recorded between 4000 cm^{-1} and 400 cm^{-1}. The resultant spectrum was inspected for spectral alterations and examined for distinctive peaks indicative of the compound's functional group.

3. Results and Discussion

3.1. Extraction and characterization of FSG

The FSG was successfully extracted using the hot extraction method (**Figure 1a**). The extract was precipitated with ethanol (**Figure 1b**); the collected precipitate was dried in a hot-air oven at below 50 ºC (**Figure 1c**). The dried extract was finely ground in a mortar and pestle and then sieved. The obtained FSG was characterized for the physical properties, and the values were tabulated in **Table 3**.

Table 3 Characterization of flaxseed gum powder

S. No.	Parameters	FSG
1	Percentage of yield	6.8%
2	Swelling index (%)	135.353±1.43
3	Viscosity (1% w/v)	108.563±0.1908 (cps)
4	Angle of repose	31.42±2.088
5	Hydration capacity	2.423±0.0294
6	Density (1) bulk density (2) tapped density	0.651±0.0721 0.788±0.0246
7	Carr's index	12.823±0.288
8	Moisture sorption capacity (%)	5.33±0.577

This open-access article is distributed under the terms of the Creative Commons Attribution Non Commercial 4.0 License (CC BY-NC 4.0).

Figure 1. Mucilage obtained after hot extraction (a), precipitated by ethanol (b), dry powder (c)

The FSG obtained via the hot extraction method shows optimal properties for SD formulations to use as carriers**.** The FSG percentage yield is 6.8%. The ring formation at the junction, following the addition of Molisch's reagent and then sulphuric acid, indicated the presence of carbohydrates in the extract. During the extraction process, fats were removed by ethanol, whereas amino acids and tannins were undetectable. It confirms the purity of gum [31]. The hot extraction procedure resulted in a 6.8% yield of gum. Linseed mucilage was separated by precipitation with n-hexane, acetone, and menthol, yielding 6.2, 6.5, and 7.0%, respectively. Linseed mucilage generated a 3-9 % yield when ultrasonicated [18]. Hot water extraction excludes the use of organic solvents commonly used to precipitate the extract; hence, toxicity associated with unwanted solvents is avoided. Ethanol effectively extracted the gum by precipitating the polysaccharides from the aqueous extract, thereby reducing the solubility of hydrophilic components. The swelling index, denoted by SI, is a crucial parameter that indicates a gum's capacity to absorb water and expand. A 135 percent swelling index for flaxseed gum indicates its substantial water-retention capacity, making it effective in improving the solubility of poorly soluble medications. The presence of hydrophilic polysaccharides in flaxseed gum enables optimal moisture and hydration capacities. All other estimated parameters of FSG were within optimal levels, making FSG suitable for enhancing the solubility of poorly soluble ATS. The solubility of ATS was increased from 310.2±0.23 µg/mL to 412.3±0.16 µg/mL through the use of solvent evaporation in the SD technique. A solid dispersion is an effective method for improving the solubility and dissolution of poorly water-soluble pharmaceuticals.

3.2. Basic physicochemical composition of FSG

Usually, a higher percentage of protein is found in gums, but it's worth noting that our reported method removed protein to a much lower level, yielding 0.47%. The differences in protein impurity levels could be due to variations in the extraction and purification procedures [32]. The moisture content of FSG was 8.1%. Flax gum with diverse moisture content has been reported in the literature [33]. The fat content of FSG was 0.4%; the reduction in fat content is actually attributed to the gum purity. The ash content was found to be 0.88%, indicating low contamination from soil, sand, and other inorganic matter. FSG was found to contain 88% of the total carbohydrates. FSG is a polysaccharide, and the percentage will vary with the extraction conditions [34].

3.2. Screening of SD formulation parameters by RSM

The amount of FSG, the volume of ethanol, and the temperature were optimized statistically using RSM. A central composite design was developed with three factors at two levels each [29]. The experimental design matrix and the results of CCD analysis are given in **Table 4**. The following regression equation (8) was obtained.

$$\text{Drug release in 30 minutes (\%) } (Y) = 64.57 + 0.9000A + 2.40B - 0.8000C - 9.18A^2 - 3.68B^2 - 4.68C^2 - 1.000AB + 0.000AC - 0.7500BC \quad (8)$$

Y is the predicted % of drug release. The effects of process parameters were demonstrated using analysis of variance (ANOVA). The regression coefficients, P, and F values are shown in **Table 4**. The model F value of 71.06 implies the model is significant. There is only a 0.01% chance that an F-value this large could occur due to noise. P-values less than 0.05 indicate model terms are

This open-access article is distributed under the terms of the Creative Commons Attribution Non Commercial 4.0 License (CC BY-NC 4.0).

significant. In this case, B, A^2, B^2, C^2 are significant model terms. Values greater than 0.1000 indicate the model terms are not significant. Model terms (A, B, C, A2, B2, C2) were found to be significant at probabilities less than 0.05, while model terms (AB, BC, AC) were found to be non-significant at probabilities greater than 0.1. The predicted R^2 of 0.8170 was in reasonable agreement with the adjusted R^2 of 0.9707, indicating the model's adequacy in predicting the response. A signal-to-noise ratio greater than 4.0 is desirable; in this case, it is 22.169. The model can thus be employed to navigate the design space, with a Lack of Fit F value of 0.637 indicating that the lack of fit is not significant compared to the pure error.

A statistically insignificant lack of fit is a strong indicator that the model equation is sufficient to predict the % of drug release accurately. The coefficient of variation (17.54% CV) indicated the precision and reliability of the model. The interaction among the components was demonstrated in **Figure 2**. Three-dimensional (3D) and two-dimensional (2D) contour plots are employed to investigate the interactions among key variables influencing the % of drug release [35], as they are straightforward and easy to interpret. Elliptical shapes indicate interaction, while circular shapes indicate no or moderate interaction between the factors [36, 37]. Interactions between the FSG and temperature and the FSG and solvent, as depicted in **Figure 2** (a1, a2, b1, b2), were found to be elliptical, indicating substantial interaction between them. The interaction between solvent and temperature, as depicted in **Figure 2** (c1, c2), exhibited a circular pattern indicating no significant impact on drug release. The combination of 33.8 mg of FSG and 8 mL of ethanol at a temperature of 42.5 °C led to a 92% release of the drug within 30 minutes. The solvent evaporation method is effective due to the molecular-level dispersion and amorphization of the drug. Best solubility of 412.3±0.16 µg/mL and dissolution rates were attained as a result of improved interactions between the drug and the polymer.

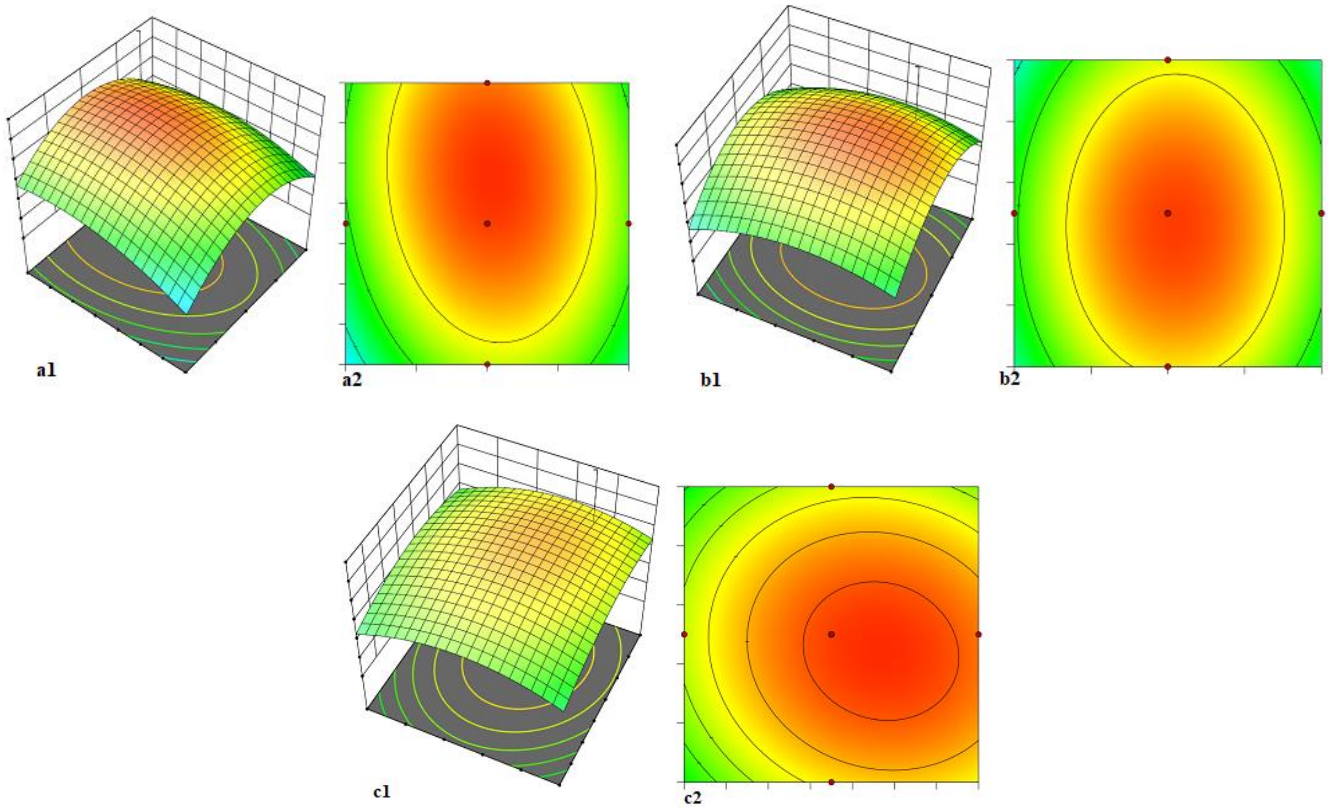

Figure 2. 3D surface and contour plots; Figure 2 (a1&a2) revealed significant interaction between carrier (FSG) and solvent, Figure 2 (b1&b2) illustrated significant interaction of carrier and temperature, Figure 2(c1&c2) indicated moderate significant interaction among solvent and temperature.

This open-access article is distributed under the terms of the Creative Commons Attribution Non Commercial 4.0 License (CC BY-NC 4.0).

Table 4 ANOVA for % of drug release in 30 minutes

Source	Sum of Squares	df	Mean Square	F-value	p-value	
Model	1247.69	9	138.63	71.06	< 0.0001	significant
A-ATR:FSG	8.10	1	8.10	4.15	0.0089	
B-SOLVENT	57.60	1	57.60	29.52	0.0003	
C-TEMPERATURE	6.40	1	6.40	3.28	0.1002	
AB	8.00	1	8.00	4.10	0.0704	
AC	0.0000	1	0.0000	0.0000	1.0000	
BC	4.50	1	4.50	2.31	0.1598	
A^2	231.84	1	231.84	118.84	< 0.0001	
B^2	37.28	1	37.28	19.11	0.0014	
C^2	60.28	1	60.28	30.90	0.0002	
Residual	19.51	10	1.95			
Lack of Fit	16.68	5	3.34	5.89	0.6371	Not significant
Pure Error	2.83	5	0.5667			
Cor Total	1267.20	19				

3.3. Characterization of SDs

Flow properties or the critical quality attributes of optimized SDs are within the acceptable limit with bulk density 0.560±0.26 g/cc, tapped density 0.654±0.16 g/cc, angle of repose 24.32±0.16, Carr's index 12.82±0.33, Hausner's ratio 1.15±0.33. ATS-SDs achieved 99-100 % of drug content with Okra gum [38]. Optimized SD was further evaluated for % EE, % yield, solubility, drug content, and % drug released after 30 minute, and the results are presented in **Table 5**.

Table 5 Characterization of SDs

Product	% EE	%Yield	Solubility	% of Drug content	Dissolution (%) after 30 minutes
SD	82	92	412.3±0.16 µg/mL	96	92

3.3.1. SEM, DSC, XRD

SEM was employed to examine the surface morphology of the optimized solid dispersion formulation. **Figure 3** depicts the SEM report. The pure drug ATS surface morphology was crystalline, as shown in **Figure 3a**, whereas the optimized formulation showed an agglomerate of ATS and did not show any crystallinity (**Figure 3b**). The size of the formulated SDs ranges from 10 µm to 64 µm. A scanning electron microscope image revealed that amorphous silver dendrites were successfully synthesised. The evaporation of the solvent can affect the shape of the prepared solid dispersions, which may subsequently impact *in vitro* dissolution rates of active pharmaceutical substances, as noted in the research by Choi and Park [39]. The results showed 98% yield, 82% entrapment efficiency, 96% drug content, and a 1.53-fold increase in solubility compared to the pure drug.

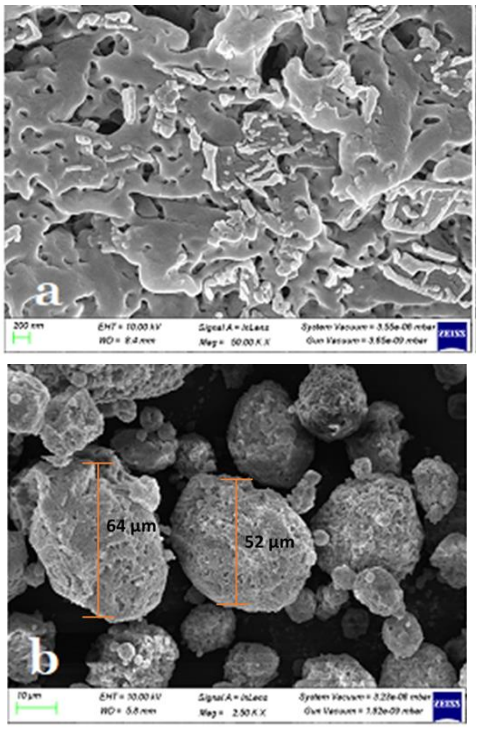

Figure 3. Pure drug ATS (a); SD Formulation (b)

This open-access article is distributed under the terms of the Creative Commons Attribution Non Commercial 4.0 License (CC BY-NC 4.0).

DSC is a valuable analytical tool for examining the thermal properties of both drugs and excipients, as well as their potential interactions within pharmaceutical formulations. Thermograms from differential scanning calorimetry can be employed to characterise the melting and crystallisation behavior of solid dispersions and the pure drug (ATS), as shown in **Figure 4**. DSC thermograms of the pure ATS drug showed two small, broad endothermic peaks at 97.7°C and 199.5°C, which represent water loss from the pure ATS. ATS have reported having about 4-6% w/w of both loosely and tightly bound water. Additionally, the DSC thermogram of ATS showed a melting endothermic peak at 158°C. The ATS-SD formulation did not exhibit the characteristic endothermic melting peak of ATS at 158°C, suggesting that ATS was present in the amorphous form in the optimized formulation. The conversion of ATS from the ordered crystalline form to the highly energetic disordered amorphous or molecularly dispersed form within the optimized ATS-SD formulation is beneficial for enhancing the ATS solubility and dissolution rate [40].

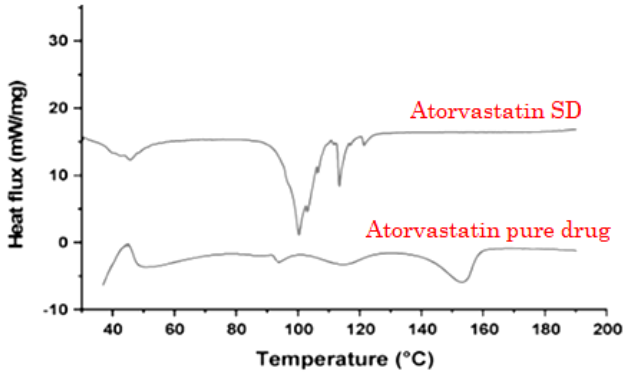

Figure 4. DSC thermograph of pure ATR and optimized SD formulation

The XRD pattern of ATS displays a large number of sharp, narrow, and intense peaks at diffraction angles of 9.01°, 18.18°, 22.32°, and 23.9°, indicating its high degree of crystallinity as shown in **Figure 5a**. The XRD spectra of FSG and SD are similar to those of a typical amorphous material and lack distinctive peaks (**Figure 5b & 5c**). The XRD pattern shown by optimum formulation indicates a decrease in the number of peaks, likely due to a reduction in crystallinity, and features broader peaks with lower intensity, suggesting a transformation of the drug from a crystalline to an amorphous form [41] (**Figure 5c**).

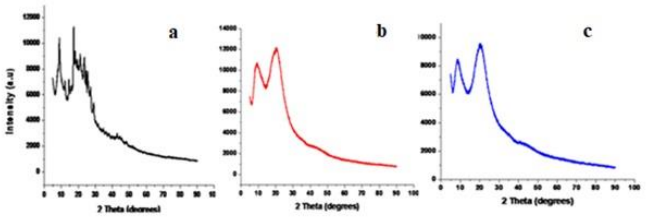

Figure 5. XRD Pattern of ATS (a), XRD Spectra of FSG (b), XRD Spectra of optimized SD.

3.3.2. Drug-excipient compatibility studies

In FTIR analysis of pure atorvastatin calcium (**Figure 6**), characteristic stretching and bending vibrations correspond to its functional groups. Here are the key peaks with approximate wave numbers (cm^{-1}). The C=O stretching 1680 cm^{-1} of ATS was reduced in intensity due to interaction with FSG. The O–H stretching 3300 cm^{-1} may become broader and stronger, indicating hydrogen bond formation in SD (**Figure7**). The C–O–C (glycosidic linkages) peak at 1100 cm^{-1} in FSG shifted due to the incorporation of ATR. Pure atorvastatin displayed a distinct peak at 3832 cm^{-1}, signifying N-H stretching. The appearance of a peak at 2441 cm^{-1} confirmed the existence of asymmetric O-H stretching vibrations, whereas the peak at 2963 cm^{-1} indicated the presence of symmetric O-H stretching. Spectral analysis reveals no alteration in the peak intensities of the drug and excipients within the formulation. It can be concluded that no interaction was observed between the drug and the excipient.

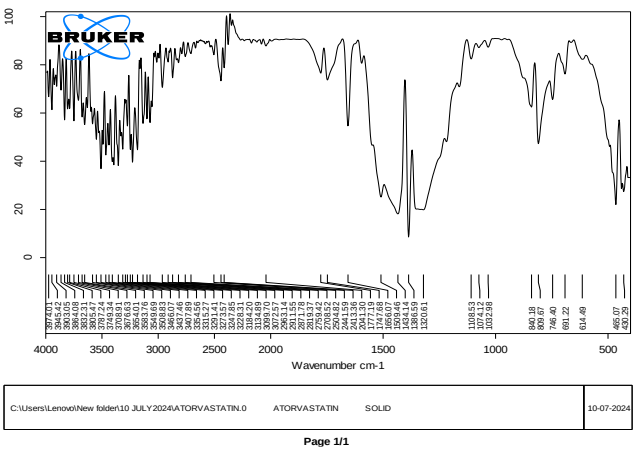

Figure 6. FTIR of Atorvastatin

This open-access article is distributed under the terms of the Creative Commons Attribution Non Commercial 4.0 License (CC BY-NC 4.0).

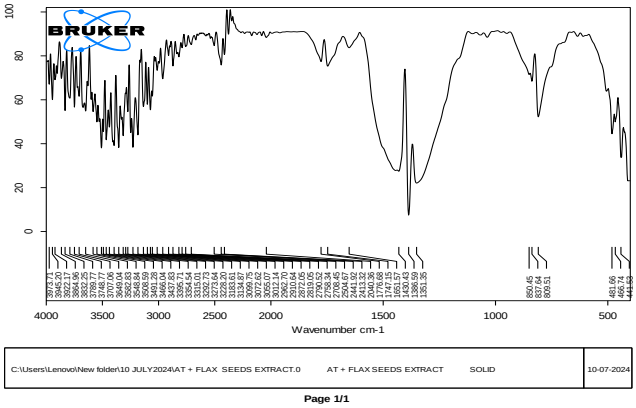

Figure 7. FTIR of solid dispersion.

In vitro dissolution profiles are consistent with those of other hydrophobic molecules when formulated as solid dispersion systems, as the transformation of the crystalline form into an amorphous form results in enhanced solubility and drug dissolution. The improved wettability provided by the FSG enabled a higher drug saturation concentration. The composition or ratio of carrier to polymer is a critical factor influencing drug encapsulation [23, 41]. Higher polymer concentrations may have boosted drug encapsulation by increasing the interaction between the drug and carrier. Similarly, there is a highly significant variation in solubility and dissolution of formulated solid dispersions due to increased wettability, reduced particle size of the drug, and reduced crystallinity of the SDs.

4. Conclusion

An aggregate of ATS-SD with FSG was formed by incorporating ATS into the FSG's polysaccharide network through solvent evaporation. Design of experiments was conducted using Response Surface Methodology (RSM) to optimize formulation parameters for SDs. 33.8 mg of FSG, 8 mL of solvent (ethanol), and 42.5°C were identified as critical quality attributes through RSM. The optimized ATR-SDs formulation exhibited 92% drug release in 30 minutes, 98% drug content, and 1.53-fold improved solubility than pure ATS. Differential scanning calorimetry and x-ray diffraction analysis showed that the drug crystalline form transformed into an amorphous state, while scanning electron microscopy images revealed increased porosity in SD. The enhancement in drug release is attributed to improved wettability of the drug particles, a considerable decrease in particle size during the formation of solid dispersions, and the presence of an amorphous form of ATS, as confirmed by DSC, FTIR, and XRD analyses. Looking back, these solid dispersions were used to develop a suitable solid dosage form formulation for improved pharmaceutical application, ultimately leading to desired release characteristics. The current research has demonstrated that the SD of ATR employing a natural carrier could be a promising formulation for enhancing solubility and dissolution.

Acknowledgment

We are grateful to the Chairman of the Vignan Group of Institutions, Dr. L. Rathaiah, for giving us bench space for this research.

Conflict of interest

The authors declared no conflict of interest.

Data availability

Data is available upon request from the corresponding author.

Authors Contributions

SSL; Conceptualization, Methodology, Writing-Original draft preparation, Software, and Supervision. BRR; Investigation, Validation. All authors read and approved the final manuscript.

Authors Orcid numbers:

Satyalakshmi S: https://orcid.org/0000-0002-1039-0036
Rama Rao B: https://orcid.org/0000-0002-5114-2872

Funding

None

Using artificial intelligence chatbots

There was no use of artificial intelligence in the making of this article.

References

1. Loftsson T, Brewster ME. Pharmaceutical applications of cyclodextrins: basic science and product development. *J. Pharm. Pharmacol.* (2010) 62: 1607-1621.

This open-access article is distributed under the terms of the Creative Commons Attribution Non Commercial 4.0 License (CC BY-NC 4.0).

2. Sun D, Gao W, Hu HX, Zhou S. Why 90% of clinical drug development fails and how to improve it? Acta Pharm. Sin. B (2022) 12: 3049-3062.
3. Patro S, Himasankar K, Choudhary AA, Rao ME. Effect of some hydrophilic polymers on dissolution rate of roxitromycin. Indian J. Pharm. Sci. (2005) 67: 334-341.
4. Rajpurohit VS, Rakha P, Goyal S, Dureja H, Arora G, Nagpal M. Formulation and characterization of solid dispersions of glimepiride through factorial design. Iran J. Pharm. Sci. (2011) 7(1): 7-16.
5. Satyalakshmi S, Sowjanya P, Kamala Kumari P. Formulation and characterization of diclofenac sodium nanogel for controlled drug release. Biosci. Biotechnol. Res. Asia (2024) 21: 967-977.
6. Siragam S, Bora RR, Nakka V, Yarraguntla SR, Kamala Kumari PV. Diclofenac sodium-curcumin nanogel: an efficient topical agent against inflammation. Indian Drugs (2024) 61(11): 30-39.
7. Mani U, Srinivasa Rao Y, Sai Sri Vastav M, Persis Joni K, Satyalakshmi S. Repurposingefavirenz for anticancer therapy with curcumin combination in solid lipid nanoparticle formulation. *Ind. J. Pharm. Edu. Res.* (2025) 59(4): 1347-1356.
8. Satya S, Rama Rao B, Karthik D, Anusha J, Kamala Kumari PV, Srinivasa Rao Y. Design, characterization, and optimization of Rosuvastatin calcium nanosponges loaded transdermal patch. Res. J. Pharm. Technol. (2024) 17(4): 1753-1757.
9. Malkawi R, Malkawi WI, Al-Mahmoud Y, Tawalbeh J. Current trends on solid dispersions past, present, and future. Adv. Pharmacol. Pharm. Sci. (2022) 2022(2): 1-17. https://doi.org/10.1155/2022/5916013
10. Budiman A, Ivana H, Huang KA, Huang SA, Nadhira MS, Rusdin A, Aulifa DL. Biocompatible natural polymer-based amorphous solid dispersion system improving drug physicochemical properties, stability, and efficacy. *Polymers* (2025) 17(15): 2059. https://doi.org/10.3390/polym17152059
11. Siragam SL. Biomedical applications of phytonanotechnology. In: Shah MP, Roy A (eds) Phytonanotechnology. Springer, Singapore (2022).
12. Ngwuluka NC, Akanbi M, Agboyo I, Uwaezuoke OJ. Characterization of gum from Sesamum indicum leaves as a suspending agent in a pediatric pharmaceutical suspension. World J. Pharm. Res. (2012) 1: 909-924.
13. Sonia TA, Sharma CP. An overview of natural polymers for oral insulin delivery. Drug Discov. Today (2012) 17(13-14): 784-792.
14. Ngwuluka NC, Ochekpe NA, Aruoma OI. Naturapolyceutics: the science of utilizing natural polymers for drug delivery. *Polymers* (2014) 6(5): 1312-1332.
15. Elleuch M, Bedigian D, Roiseux O, Besbes S, Blecker C, Attia H. Dietary fibre and fibre-rich by-products of food processing: characterisation, technological functionality and commercial applications: a review. Food Chem. (2011) 124: 411-421.
16. Liu J, Shim YY, Timothy JT, Wang Y, Reaney MJ. Flaxseed gum: a versatile natural hydrocolloid for food and non-food applications. Trends Food Sci. Technol. (2018) 75: 146-157.
17. Nasrabadi MN, Goli SA, Doost AS, Roman B, Dewettinck K, Stevens CV, Van der Meeren P. Plant-based Pickering stabilization of emulsions using soluble flaxseed protein and mucilage nano-assemblies. Colloids Surf. A Physicochem. Eng. Asp. (2019) 563: 170-182.
18. Tulain UR, Mahmood A, Aslam S, Erum A, Malik NS, Rashid A, et al. Formulation and evaluation of Linum usitatissimum mucilage-based nanoparticles for effective delivery of ezetimibe. *Int. J. Nanomedicine* (2021) 16: 4579-4596.
19. Dong W. Preparation, characterization, and in vitro/vivo evaluation of polymer-assisting formulation of atorvastatin calcium based on solid dispersion technique. Asian J. Pharm. Sci. (2018).
20. Lopusiewicz L, Dmytrow I, Mituniewicz-Małek A, Kwiatkowski P, Kowalczyk E, Sienkiewicz M, Drozlowska E. Natural gum from flaxseed by-product as a potential stabilizing and thickening agent for acid whey fermented beverages. *Appl. Sci.* (2022) 12(20): 10281. https://doi.org/10.3390/app122010281
21. Sadiq T, Khalid SH, Khan IU, Mahmood H, Asghar S. Designing deferoxamine-loaded flaxseed gum and carrageenan-based controlled release biocomposite hydrogel films for wound healing. *Gels* (2022) 8(10): 652. https://doi.org/10.3390/gels8100652
22. Ramteke S, Haigune N, More S, Pise S, Pise A, Kharwade R. Flaxseed mucilage hydrogel based floating drug delivery system: design and evaluation. Res. J. Pharm. Technol. (2022) 15(4): 1549-1554. https://doi.org/10.52711/0974-360X.2022.00258
23. Faraji E. Development of the binary and ternary atorvastatin solid dispersions: in vitro and in vivo investigations. Biomed. Res. Int. (2021). https://doi.org/10.1155/2021/
24. Elmowafy M. Atorvastatin-loaded nanostructured lipid carriers (NLCs): strategy to overcome oral delivery drawbacks. *Drug Deliv.* (2017) 24: 932-941. https://doi.org/10.1080/10717544.2017.

This open-access article is distributed under the terms of the Creative Commons Attribution Non Commercial 4.0 License (CC BY-NC 4.0).

25. Farooq U, Malviya R, Sharma PK. Extraction and characterization of okra mucilage as pharmaceutical excipient. Acad. J. Plant Sci. (2013) 6: 168-172.
26. Safdar B, Pang Z, Liu X, Jatoi MA, Mehmood A, Rashid MT, Ali N, Naveed M. Flaxseed gum: extraction, bioactive composition, structural characterization, and its potential antioxidant activity. J. Food Biochem. (2019) 44(2): e13158. https://doi.org/10.1111/jfbc.13158
27. Mallikarjun PN, Satyalakshmi S, Jyothsna P, Srinivasa Rao Y. Rosuvastatin calcium nanosponges in the formulation of extended-release tablets. Indian Drugs (2021) 58(10): 25-33.
28. Rashid F, Ahmed Z, Hussain S, Huang JY, Ahmad A. Linum usitatissimum L. seeds: flax gum extraction, physicochemical and functional characterization. *Carbohydr. Polym.* (2019) 215: 29-38. https://doi.org/10.1016/j.carbpol.2019.03.054
29. Lakshmi SS, Mahesh CH, Gayatri K, Manisha P, Aishwarya K. Statistical optimization of amylase production and its purification from a palm wine isolate Bacillus sp., Q-164. Biocatal. Agric. Biotechnol. (2020) 29: 101784.
30. Torrado-Salmeron C, Guarnizo-Herrero V, Torrado G, Peña MA, Torrado-Santiago S, de la Torre-Iglesias PM. Solid dispersions of atorvastatin with Kolliphor RH40: enhanced supersaturation and improvement in a hyperlipidemic rat model. Int. J. Pharm. (2023) 631: 122520.
31. Yadav RNS, Agarwala M. Phytochemical analysis of some medicinal plants. J. Phytol. (2021) 3: 12-19.
32. Dong X, Rawiwan P, Middleditch M, Guo G, Woo MW, Quek SY. Effects of protein variations by different extraction and dehydration approaches on hempseed protein isolate: protein pattern, amino acid profiling and label-free proteomics. *Food Chem.* (2024) 460: 137145.
33. Puligundla P, Lim S. A review of extraction techniques and food applications of flaxseed mucilage. *Foods* (2022) 11(12): 1677. https://doi.org/10.3390/foods11121677
34. Ansari S. Determination of protein, fat, fibre, WAI, moisture and ash. (2022).
35. Satyalakshmi S, Girija Shankar G, Prabhakar T, Satish T. Statistical optimization of keratinase production from marine fungus. *Int. J. Eng. Res. Appl.* (2015) 5(2): 52-58.
36. Gajdhane SB, Bhagwat PK, Dandge PB. Response surface methodology-based optimization of production media and purification of α-galactosidase in solid-state fermentation by Fusarium moniliforme NCIM 1099. 3 Biotech (2016) 6: 1-14.
37. Bhagwat PK, Bhise KK, Bhuimbar MV, Dandge PB. Use of statistical experimental methods for optimization of collagenolytic protease production by Bacillus cereus strain SUK grown on fish scales. Environ. Sci. Pollut. Res. (2018) 25: 28226-28236.
38. Alghadi RY, Abdel Kareem AM, Abuelrakha ABS, Alqamar MO, Ibrahim BA. In vitro and in vivo assessment of the effect of okra gum solid dispersion in atorvastatin solubility. Saudi J. Med. Pharm. Sci. (2024) 10(1): 37-46.
39. Choi JS, Park JS. Design of PVP/VA S-630 based tadalafil solid dispersion to enhance the dissolution rate. *Eur. J. Pharm. Sci.* (2017) 97: 269-276.
40. Slamova M, Skolakova T, Skolakova A, Patera J, Zamostny P. Preparation of solid dispersions with respect to the dissolution rate of active substance. *J. Drug Deliv. Sci.* Technol. (2020) 56: 101518.
41. Reza G, Mohammad MM. Formulation and evaluation of atorvastatin tablets by solid dispersion technique. *Acta Pharm. Sci.* (2023) 61(3): 285-302.

This open-access article is distributed under the terms of the Creative Commons Attribution Non Commercial 4.0 License (CC BY-NC 4.0).